A Novel Method for Quantifying Value in Spaceborne Soil Moisture Retrievals

WADE T. CROW

Hydrology and Remote Sensing Laboratory, USDA Agricultural Research Service, Beltsville, Maryland

ABSTRACT

A novel methodology is introduced for quantifying the added value of remotely sensed soil moisture products for global land surface modeling applications. The approach is based on the assimilation of soil moisture retrievals into a simple surface water balance model driven by satellite-based precipitation products. Filter increments (i.e., discrete additions or subtractions of water suggested by the filter) are then compared to antecedent precipitation errors determined using higher-quality rain gauge observations. A synthetic twin experiment demonstrates that the correlation coefficient between antecedent precipitation errors and filter increments provides an effective proxy for the accuracy of the soil moisture retrievals themselves. Given the inherent difficulty of directly validating remotely sensed soil moisture products using ground-based observations, this assimilation-based proxy provides a valuable tool for efforts to improve soil moisture retrieval strategies and quantify the novel information content of remotely sensed soil moisture retrievals for land surface modeling applications. Using real spaceborne data, the approach is demonstrated for four different remotely sensed soil moisture datasets along two separate transects in the southern United States. Results suggest that the relative superiority of various retrieval strategies varies geographically.

1. Introduction

Despite significant advances in the development of remote sensing techniques for surface soil moisture, objective quantification of value for soil moisture retrievals remains an elusive goal. Traditional remote sensing product validation is based on the direct intercomparison of retrieved quantities with, presumably higher-accuracy, ground-based measurements. Significant progress has been made in the design of field experiments and operational networks that facilitate the up-scaling of point-scale soil moisture ground observations to a spatial support comparable to the resolution of spaceborne microwave radiometers (Jackson et al. 1999; Famiglietti et al. 1999; Jacobs et al. 2004; Cosh et al. 2004). However, these approaches are still generally limited in space (by the extent of the network) and/or time (by the length of the field experiment).

A broader view of assigning value to remote sensing retrievals also requires that some consideration be given to the manner in which data will be utilized in higher-order applications. A key application for remotely sensed soil moisture retrievals is their assimilation into land surface models at the core of atmospheric and hydrologic prediction systems (Leese et al. 2001). A robust determination of value for remote sensing observations in modeling applications should reflect our ability to obtain comparable information from other observational resources. For global soil moisture products, the fundamental issue is how much marginal value retrievals add to model-based soil moisture estimates above and beyond what is obtainable from water balance modeling using globally available precipitation products (Crow et al. 2005a). Past work has demonstrated the potential for enhancing soil moisture predictions from global land surface models using spaceborne soil moisture products (Reichle and Koster 2005), but such efforts are generally hampered by limitations in the availability and accuracy of ground-based soil moisture observations.

Here we propose an alternative methodology for quantifying the value of soil moisture remote sensing retrievals for global land surface modeling applications. The approach is based on the assimilation of remotely sensed soil moisture retrievals into a simple linear wa-

Corresponding author address: W. T. Crow, Hydrology and Remote Sensing Laboratory, USDA Agricultural Research Service, Rm. 104, Bldg. 007, BARC-W, Beltsville, MD 20705.
E-mail: wcrow@hydrolab.arsusda.gov

ter balance model (driven by satellite-based global precipitation products) using a standard Kalman filtering methodology. The novelty of the approach originates not from its simple data assimilation and modeling methodology, rather the manner in which filtering results are subsequently interpreted. Specifically, filter increments (discrete additions or subtractions of water suggested by the filter in response to soil moisture retrievals) are compared to antecedent rainfall errors—calculated as the difference between currently available global precipitation products and higher-quality gauge-based products available only in precipitation data–rich areas of the globe. The correlation between past rainfall errors and current filter increments reflects the ability of the soil moisture retrievals to add value to model-based soil moisture estimates obtained using currently available global precipitation products. Our central hypothesis is that the strength of this correlation can be interpreted as a robust proxy for the added value of spaceborne soil moisture in global modeling applications and therefore provides valuable feedback information for developers of spaceborne soil moisture products.

If verified, the advantage of this approach over traditional validation techniques would be twofold. First, it would provide a framework for quantifying the value-added information content in remote sensing observations. That is, its utility above and beyond soil moisture information that is currently available from analysis of global precipitation products. In addition, it would allow any precipitation data–rich area of the globe (e.g., the contiguous United States) to be treated as a continental-scale test bed site for quantifying the value of spaceborne soil moisture retrievals over the larger fraction of the globe that is precipitation data–poor. Currently such test beds are limited to relatively sparse space and time periods in which sufficiently dense ground-based soil moisture observations are available.

Section 2 describes the datasets and study sites employed in the analysis. The development of the data assimilation–based approach is described in section 3. Section 4 tests the proposed approach using synthetically generated remote sensing observations, and section 5 uses the approach to establish a large-scale test bed in the southern United States in which four separate spaceborne soil moisture datasets are evaluated.

2. Data and study sites

Two separate daily precipitation datasets are used in the analysis. Satellite-based precipitation products are taken from the one latitude–longitude degree daily (1DD) Global Precipitation Climatology Project (GPCP) rainfall product based on infrared retrievals from the Television Infrared Observation Satellite (TIROS) Operational Vertical Sounder (TOVS) and the Geostationary Operational Environmental Satellite (GOES) and passive microwave measurements from the Special Sensor Microwave Imager (SSM/I) (Huffman et al. 2001). Over some continental areas, GPCP-1DD monthly rainfall totals are corrected to match sparse ground-based observations (Huffman et al. 2001). However, at finer time scales the product relies exclusively on satellite-based precipitation estimates. For many areas of the world, such satellite-based products represent the best available source of precipitation data. Nevertheless they are prone to error, especially over land (McPhee and Margulis 2005). The second precipitation dataset is the National Centers for Environmental Prediction's (NCEP's) Climate Prediction Center (CPC) retrospective rainfall product over the contiguous United States. The product is based on combining CPC real-time rain gauge observations with those from available non-real-time networks to yield approximately 13 000 rain gauge observations of daily rainfall. Following the approach of McPhee and Margulis (2005), CPC data processed as part of the North American Land Data Assimilation System (NLDAS) project (see Cosgrove et al. 2003) is aggregated into a daily (0000–0000 UTC) 1° latitude–longitude product to match the temporal and spatial attributes of the GPCP-1DD dataset. As noted by McPhee and Margulis (2005), CPC-based daily rainfall products derived in this manner likely represent the best currently available estimate of daily rainfall accumulations within the contiguous United States.

Four separate remotely sensed soil moisture datasets are also considered in the analysis. The first two are based on X-band (10.6 GHz) brightness temperature (T_B) observations from the Tropical Rainfall Measuring Mission (TRMM) Microwave Imager (TMI) and the soil moisture datasets described in Bindlish et al. (2003) (TMI_{USDA}) and Gao et al. (2006) (TMI_{LSMEM}). The TMI_{LSMEM} product is based on application of the Land Surface Microwave Emission Model (LSMEM) described in Drusch et al. (2001) and Gao et al. (2004). TMI X-band T_B observations are available on a roughly daily basis since late 1997 and have a ground-based spatial resolution of approximately 38^2 km^2. Because of TRMM orbital characteristics, observations are available only for the latitude band between 40° north and south. The second two soil moisture products are based on the application of the LSMEM (AMSR-E$_{LSMEM}$) and Njoku et al. (2003) retrieval approaches to X-band
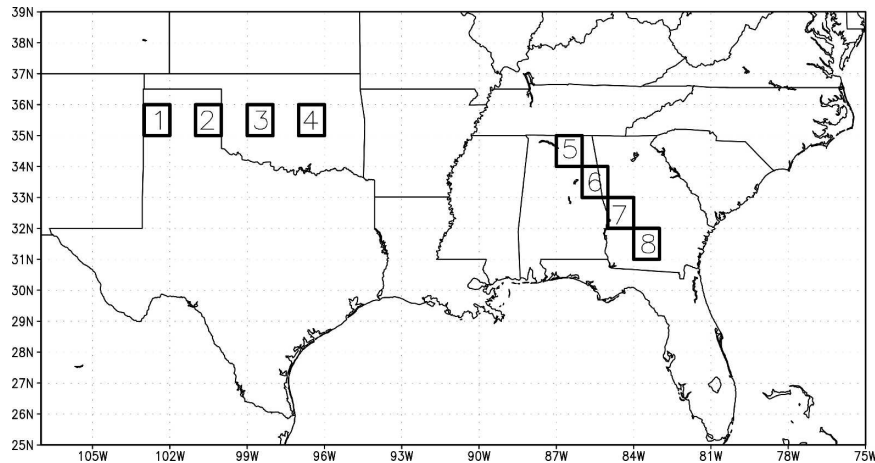
FIG. 1. Location of 1° lat–lon study boxes. Boxes 1–4 are referred to as the Texas/Oklahoma (TX/OK) transect. Boxes 5–8 are referred to as the Alabama/Georgia (AL/GA) transect.

observations obtained from the Advanced Microwave Scanning Radiometer (AMSR-E) aboard the National Aeronautics and Space Administration (NASA) *Aqua* satellite. The Njoku et al. (2003) algorithm provides the basis of the official NASA level 3 AMSR-E soil moisture product (AMSR-E$_{NASA}$). The algorithm has been modified from its original form to eliminate reliance on C-band observations corrupted by large amounts of radio frequency interference over the United States (E. Njoku 2006, personal communication). AMSR-E X-band T_B observations have been globally available since mid-2002 with a global repeat time of 2 to 3 days and spatial resolution of approximately 40^2 km^2. All soil moisture products were aggregated in time and space to form a daily 1° latitude–longitude soil moisture product consistent with the GPCP-1DD rainfall product.

The analysis will focus on the eight 1° latitude–longitude boxes shown in Fig. 1. The first four boxes stretch from the panhandle area of Texas (TX) into central Oklahoma (OK) and will be referred to as the "TX/OK transect." This transect samples across a strong precipitation and vegetation gradient with semi-arid shrublands prevailing in the west (box 1) and more humid, and densely vegetated, cropland and forest cover emerging along its eastern edge (box 4). The other four boxes span an area of the southeastern United States from northern Alabama (AL) to south-western Georgia (GA) and will be referred to as the "AL/GA transect." Relative to the TX/OK transect, denser vegetation and more pronounced topography within the AL/GA transect present a greater challenge for soil moisture remote sensing. Land cover is generally a mixture of forested upland areas, crops (corn, soybean, peanuts, and cotton), and pasture.

3. Methodology

The methodology is based on a simple antecedent precipitation index (API) approach to water balance modeling. Here, API for day i is defined as

$$API_i = \gamma API_{i-1} + P_i, \qquad (1)$$

where P_i is satellite-based GPCP-1DD precipitation and γ is the API loss coefficient. The API model is applied separately to each of the 1° latitude–longitude boxes shown in Fig. 1. For simplicity, γ is set equal to 0.85 for all boxes. The impact of error in the specification of γ is addressed in section 4a.

a. Kalman filtering

For linear forecasting models with Gaussian errors, a Kalman filter provides the optimal method of updating the expectation and error covariance of a model state forecast (e.g., API) with noisy observations (e.g., remotely sensed soil moisture retrievals θ_{RS}). The first step in this process is defining a measurement operator capable of converting θ_{RS} retrievals into API values. Here the operator is defined by calculating a least squares regression line (with slope b and intercept a) for the observed long-term relationship between API and θ_{RS}. Separate regression relationships are calculated for each of the 1° latitude–longitude boxes shown in Fig. 1. However, data within each box are temporally lumped and potential seasonal variability is neglected. Unlike (1), API values used to define this relationship are derived from the gauge-based CPC rainfall product.

Using a and b defined by these regression relationships, the Kalman filters predicts that the optimal updating of expected API at time i—based on the simultaneous observation of θ_{RS}—is given by

$$\text{API}_i^+ = \text{API}_i^- + K_i(\theta_{\text{RS}_i} - a - b\text{API}_i^-), \quad (2)$$

where K is the Kalman gain

$$K_i = bT_i^-/(b^2T_i^- + S), \quad (3)$$

T is the dynamic error in model-predicted API, and S is the error in θ_{RS} retrievals. The "$-$" and "$+$" symbols in (2) and (3) reflect quantities before and after updating, respectively. The update equation in (2) relates the magnitude of changes in API soil moisture budgeting warranted by consideration of θ_{RS} observations. These updates, $K_i(\theta_{\text{RS}_i} - a - b\,\text{API}_i^-)$, are commonly referred to as "analysis increments." The Kalman gain K describes how optimal choices for increments depend on the magnitude of b, T, and S. Note how either large observation error (S) or a lack of sensitivity between observations and model states (low b) are associated with small analysis increments (low K). Conversely, larger model forecast uncertainty T or lower observation error S increases K and leads to larger adjustments to API via (2). Since the availability of observations reduces uncertainty in API forecasts, model forecast error T is also adjusted at measurement times via

$$T_i^+ = (1 - bK_i)T_i^-. \quad (4)$$

Between soil moisture observations, and the adjustment of API and T via (2) and (3), the model state API is temporally updated using observed P and (1). In parallel, model forecast error T is updated in time following

$$T_i^- = \gamma^2 T_{i-1}^+ + Q, \quad (5)$$

where Q relates the uncertainty added to an API forecast as it is propagated from time $i - 1$ to i.

Selecting appropriate values for the observation variance S in (3) and the forecast noise parameter Q in (5) is often a challenging aspect of Kalman filtering. An important diagnostic tool for addressing this problem is the statistical analysis of filter innovations, $\theta_{\text{RS}_i} - (a + b\text{API}_i^-)$, encountered when applying (2) (Reichle et al. 2002). For fully linear systems where Q and S are correctly specified, implementation of the Kalman filter will lead to a temporal sequence of normalized filter innovations

$$\alpha_i = [\theta_{\text{RS}_i} - (a + b\text{API}_i^-)]^2/(b^2T_i^- + S) \quad (6)$$

that are mean one (Dee 1995).

The overall Kalman filter analysis stream goes as follows. Magnitudes of API and T are initialized at some default value and are propagated to the first observation time using (1) and (5). At this time, API and T are updated for the impact of observed θ_{RS} using (2) and

(4). Updated T and API values are then temporally repropagated using (1) and (5) until the next observation time and the cycle is repeated. For calibration of synthetic filtering results presented in section 4, S is assumed known and the magnitude of Q is adjusted until filtering leads to a normalized innovation (α) sequence with a mean of one. Both Q and S are considered constant in time. Additional calibration details for real-data cases presented in section 5 are discussed in section 4b.

While the execution of the filter via (1)–(5) can appear somewhat involved, its role in this analysis is very straightforward. The Kalman filter simply presents an optimal methodology whereby water can be added or subtracted from API predictions in response to the availability of surface soil moisture observations. By considering relative errors in both model forecasts (T) and the remotely sensed observations (S), the filter makes these updates in such a way that the error in API forecasts is minimized.

b. Definition of R_{value}

Kalman filter analysis increments, defined via (2) as $K_i(\theta_{\text{RS}_i} - a - b\text{API}_i^-)$, describe the depth of water added or subtracted from the API model in the course of assimilating θ_{RS}. If θ_{RS} retrievals are minimally accurate and the filter properly constructed, these increments should correlate in some manner with antecedent rainfall forcing errors. Specifically, positive (negative) rainfall errors should lead to the removal (addition) of water in the near future. The availability of high-quality rain gauge observations for precipitation data–rich areas like the contiguous United States provides a means by which the quality of updates made to an API model (driven by poor-quality GPCP-1DD daily rainfall) via the assimilation of remotely sensed observations can be evaluated. This, in turn, opens up the possibility of using precipitation data–rich areas as a large-scale test beds for remotely sensed surface soil moisture products.

Figure 2 demonstrates basic aspects of the approach using the TMI$_{\text{LSMEM}}$ soil moisture product. For a period of time in spring 2003, Fig. 2a displays total daily GPCP-1DD and CPC rainfall estimates (see section 2) for the 1° latitude–longitude box centered at 35.5°N, −102.5°W (box 1 in Fig. 1). Note how, relative to the more accurate CPC product, the satellite-based GPCP-1DD rainfall retrieval underestimates the magnitude of a rainfall event on 19–20 March and subsequently overestimates rainfall for a 27–29 March event. Forcing an API model with GPCP-1DD precipitation (Fig. 2b) produces an API prediction (Fig. 2b) at odds with the TMI$_{\text{LSMEM}}$ θ_{RS} retrieval (Fig. 2c), which echoes the
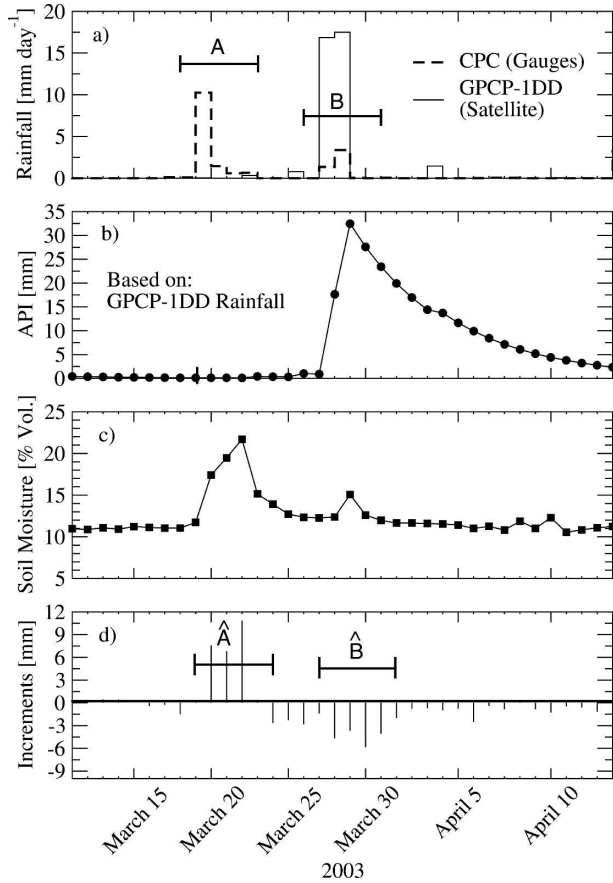
FIG. 2. Times series of daily (a) rainfall, (b) GPCP-1DD API, (c) remotely sensed soil moisture (TMI$_{\mathrm{LSMEM}}$), and (d) Kalman filter increments during 2003 for box 1 in Fig. 1.
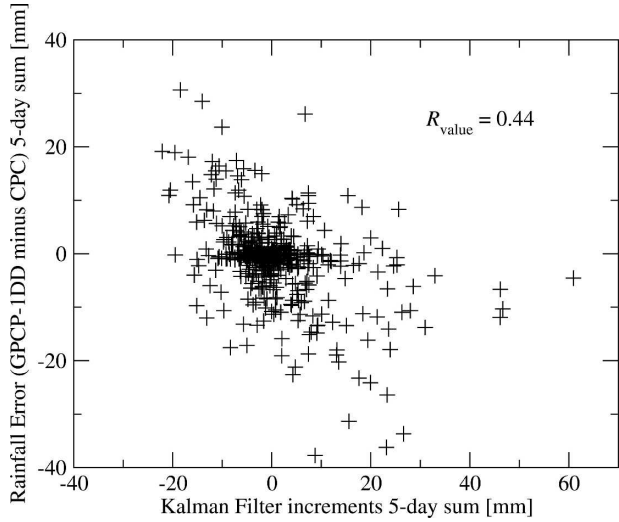

FIG. 3. For box 1 in Fig. 1 between 1998 and 2004, scatterplot of rainfall errors (5-day sums) vs Kalman filter analysis increments (5-day sums lagged by 1 day) associated with assimilating TMI$_{\mathrm{LSMEM}}$ soil moisture retrievals into an API model; R_{value} is defined to be the opposite (i.e., negative) of the Pearson correlation coefficient for the plot 2.

CPC rainfall data in suggesting that the 19–20 March storm was the larger of the two events. Consequently, the assimilation of θ_{RS} into the API model (Fig. 2b) leads to the Kalman filter analysis increments plotted in Fig. 2d. Note the inverse relationship between 5-day rainfall errors (during periods A and B in Fig. 2) and subsequent 5-day sums of analysis increments (during periods Â and B̂ in Fig. 2d, which lag A and B in Fig. 2a by a single day). Underestimation (overestimation) of precipitation accumulations during period A (B) is followed by the addition (subtraction) of water by the filter during period Â (B̂). This inverse relationship between precipitation accumulation errors and subsequent increment depths suggests that the assimilation of θ_{RS} is adequately compensating API predictions for deficiencies in the GPCP-1DD precipitation product. Over longer periods of time, this relationship manifests itself as a negative correlation between 5-day sums of rainfall errors and filter innovations. For box 1 in Fig. 1, Fig. 3 shows a scatterplot of 5-day (pentad) sums of rainfall errors and filter increments (lagged by 1 day)

for the TMI$_{\mathrm{LSMEM}}$ dataset during the calendar years from 1998 to 2004. Here and throughout the analysis, only pentads in which either CPC or GPCP-1DD rainfall products estimate nonzero rainfall accumulations are considered. The negative of the standard Pearson correlation coefficient (R) calculated for the relationship in Fig. 3 will subsequently be referred to as the R_{value} coefficient for a particular remotely sensed soil moisture product:

$$R_{\mathrm{value}} = -R. \tag{7}$$

Simply stated, this R_{value} metric reflects the degree to which temporal API adjustments, made by the Kalman filter in response to uncertain θ_{RS} observations, are correlated with antecedent errors in precipitation products used to calculate API.

4. Synthetic twin experiment analysis

The magnitude of the negative correlation seen in Fig. 3 reflects the ability of a remotely sensed soil moisture product (and the Kalman filter) to detect (and correct) soil moisture modeling errors arising from the use of noisy precipitation inputs. Our central hypothesis is that the strength of this correlation can be used as a robust proxy for the overall information content of remotely sensed surface soil moisture in global land surface modeling applications. To test this assumption, we utilize a synthetic twin methodology where a bench-

mark "truth" simulation of surface soil moisture values is synthetically generated using an API modeling approach. These benchmark soil moisture values are then artificially perturbed with random noise to simulate remote sensing observations and reassimilated back into the API model following section 3. Such experiments are referred to "synthetic twin experiments" in the data assimilation literature where they are commonly used to test assumptions underlying the application of data assimilation procedures (e.g., Reichle et al. 2002). Unlike real-data cases, the availability of "truth" soil moisture in a synthetic twin experiment allows for the explicit calculation of the Pearson correlation coefficient between the benchmark soil moisture and the remotely sensed soil moisture retrieval (R_{truth}).

Seven years of CPC and GPCP-1DD rainfall data from the TX/OK transect are used to force a series of synthetic experiments. Using the Kalman filter approach outlined in section 3 and the synthetically derived soil moisture observations, R_{value} magnitudes are calculated following Fig. 3 and (7) for a large number of cases in which the magnitude of artificial noise added onto "truth" soil moisture to obtain synthetic observations is systematically varied. In addition, various levels of rainfall accuracy are obtained by subtracting the GPCP-1DD (satellite based) precipitation time series for a particular 1° latitude–longitude box from the equivalent CPC (gauge based) time series, multiplying the difference by a constant ranging between 0.5 and 2.0 (see legend in Fig. 4), and then adding the scaled difference time series back to the CPC daily rainfall time series.

Figure 4 summarizes results from these synthetic experiments; R_{truth} values plotted on the x axis of Fig. 4 reflect the Pearson correlation coefficient calculated between "truth" soil moisture (synthetically generated using API modeling) and soil moisture observations (generated by adding artificial Gaussian noise to "truth" soil moisture). While such correlations provide an effective means of summarizing the overall value of soil moisture remote sensing observations for land surface modeling applications (Crow et al. 2005b), a lack of ground-based soil moisture observations and the coarse-spatial resolution of spaceborne retrievals hampers their accurate calculation in most real-world cases. In contrast, R_{value} magnitudes on the y axis can be estimated anywhere relatively accurate gauge-based precipitation observations are available. Except for very high retrieval accuracies, a monotonic relationship trending through the plot origin exists between R_{value} and R_{truth} for all assumed rainfall accuracies. This suggests that R_{value} provides a robust and readily observable proxy for less readily available R_{truth} magnitudes.
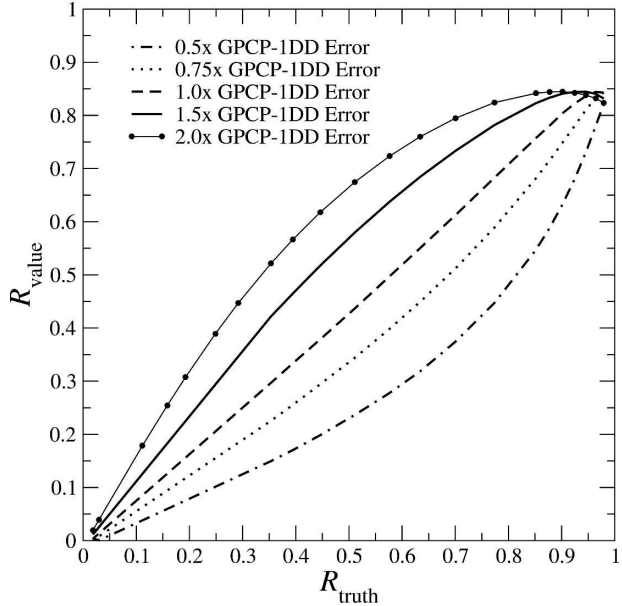

FIG. 4. For the synthetic twin experiment, the relationship between R_{value}, rainfall accuracy (various lines), and the Pearson correlation coefficient between true and retrieved soil moisture (R_{truth}).

In addition, the size of R_{value} provides a meaningful representation of added value contributed by remote sensing retrievals, that is, improvements in soil moisture accuracy above and beyond that obtainable from a water balance approach driven by observed precipitation. For the same R_{truth}, R_{value} decreases (increases) with increasing (decreasing) GPCP-1DD rainfall accuracy. Reflecting that as the accuracy of satellite-based global rainfall products increases, it becomes increasingly difficult to contribute added value to model-predicted soil moisture. In this way R_{value} provides a metric of added value that is sensitive to both retrieval uncertainty as well as the accuracy of competing model-based soil moisture estimates derived without soil moisture remote sensing or data assimilation.

a. Sensitivity to nonidealized conditions

Admittedly, Fig. 4 captures only idealized conditions within a synthetic experiment. In reality, a number of additional factors complicate the interpretation of R_{value}. First, while typically considered the highest-quality rainfall observations available in the contiguous United States (McPhee and Margulis 2005), CPC rainfall products are not, of course, truly error free. Figure 5a demonstrates the impact on R_{value}, for the $1.0 \times$ GPCP-1DD rainfall error case in Fig. 1, of errors in the CPC rainfall dataset used as a benchmark for the calculation of rainfall errors. Here rainfall uncertainty is
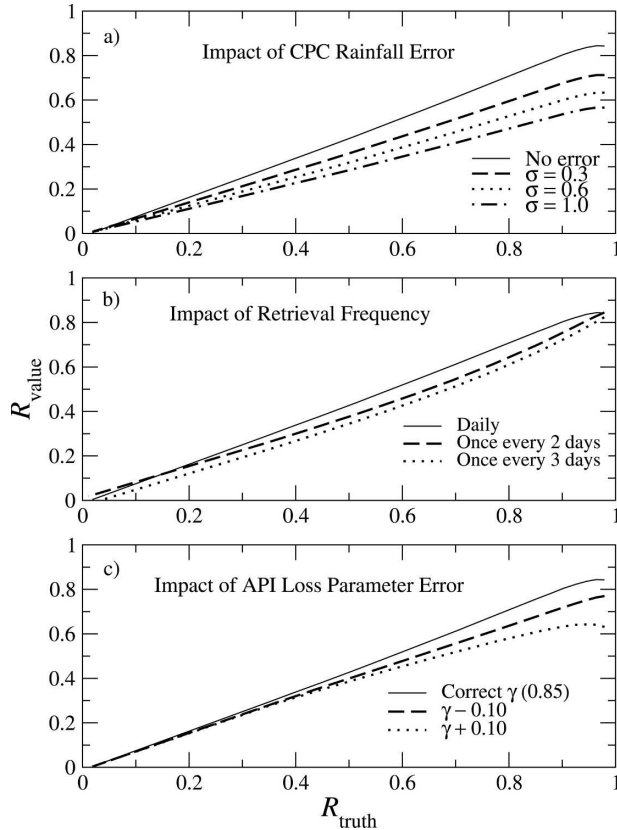
FIG. 5. Sensitivity of the $1.0 \times$ GPCP-IDD error line in Fig. 4 to (a) error in the CPC rainfall data assumed as a benchmark, (b) temporal subsampling of synthetically generated soil moisture retrievals, and (c) errors in the specification of the API loss coefficient γ in (1).

FIG. 6. For the $1.0 \times$ GPCP-1DD and $R_{\text{truth}} = 0.75$ case in the synthetic twin experiment, relationship between the assumed measurement variance S_{assumed}, the actual variance S_{true}, and R_{value}.

represented by the application of mean-zero, lognormal multiplicative noise (with a standard deviation of σ) to CPC rainfall. The inclusion of CPC error leads to a modest reduction in R_{value} values and the sensitivity of R_{value} to variations in R_{truth}. These reductions make it marginally more difficult to establish the statistical significance of a given R_{value} coefficient and/or the difference in coefficients for two competing θ_{RS} products. However, the error does not impact the monotonic nature of its relationship with R_{truth}. In addition, since R_{value} is a correlation-based metric, CPC bias errors arising from well-known undercatch problems with ground-based rain gauges (e.g., Groisman and Legates 1994) will have no effect on its estimation. Relatively minor effects are also noted when synthetic θ_{RS} retrievals are subsampled to time to match the temporal sampling limitations of proposed spaceborne missions (Fig. 5b).

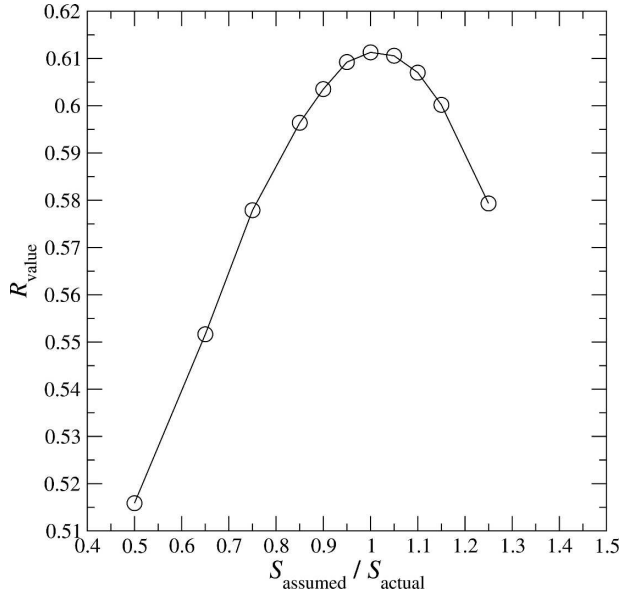From a modeling standpoint, another key simplification lies in the assumption that land surface modeling errors are due solely to the impact of poor precipitation input data. In reality a broad range of model parameterization, structural, and input errors lead to uncertainty in land surface model soil moisture predictions. For the sensitivity experiment presented in Fig. 5c, the API model used to generate synthetic observations employed a different loss coefficient than the API model used in the data assimilation procedure (see legend for differences). Consequently, results reflect the added impact of poor model parameterization on the calculation of R_{value}. While incorrect model parameterization leads of a reduction of R_{value} sensitivity for large R_{value}, the impact below $R_{\text{value}} = 0.6$ is relatively modest. Overall, while the nonidealized conditions examined in Fig. 5 can potentially reduce the sensitivity of R_{value} to R_{truth}, none of them undermine the fundamental interpretation of R_{value} as a robust proxy for R_{truth}.

b. Filter calibration

In a synthetic experiment, measurement noise S is known a priori. This allows the forecasting noise Q to be calibrated based on the sampled mean of α. In reality, S must also be estimated and there exists a range of possible S values, and corresponding Q values, for which the temporal mean of α is one. Figure 6 examines this issue from the context of our synthetic twin analysis by plotting R_{value} (for the $R_{\text{truth}} = 0.75$ and $1.0 \times$ GPCP-1DD error case in Fig. 4) for a range of assumed S. Since this is a synthetic experiment, the correct observation error (S_{true}) is known and can be used to

normalize assumed S values ($S_{assumed}$). For each choice of $S_{assumed}$, forecast error Q is individually calibrated so that the α time series is mean one. Synthetic results plotted in Fig. 6 demonstrate that while R_{value} exhibits some sensitivity to $S_{assumed}$, the largest R_{value} is associated with $S_{assumed} = S_{true}$. Consequently, when considering a range of potential S and Q combinations, each producing a mean-unity α time series, the correct choice will be the S value that also maximizes R_{value}. This additional constraint allows S and Q to be uniquely defined and is used to calibrate the approach for real-data cases examined in section 5.

5. Real-data analysis

The relationship plotted in Fig. 4 suggests two primary applications for R_{value} estimates. First, if R_{value} is statistically greater than zero within a test bed location, it demonstrates that remotely sensed soil moisture retrievals are adding value to soil moisture estimates derived from water balance modeling and global rainfall products. The use of precipitation data–rich areas as test bed sites can improve our ability to predict the global extent of land cover types over which remotely sensed soil moisture contributes value to land surface modeling. Second, for a given test bed site, statistically significant differences in R_{value} magnitudes for two (or more) competing soil moisture products demonstrates that a particular retrieval algorithm is providing a more valuable representation of soil moisture dynamics. Based on Fig. 4, larger R_{value} coefficients can be interpreted as reflecting higher accuracy in soil moisture retrievals and greater value for land surface modeling applications. This feedback can, in turn, can be exploited to optimize soil moisture retrieval algorithms.

Figure 7 shows R_{value} results for AMSR-E soil moisture datasets described in section 2 over the eight 1° latitude–longitude boxes shown in Fig. 1. Since AMSR-E observations are available once every 2–3 days, only 5-day periods containing at least three AMSR-E observations are used to calculate R_{value}. Plotted results are based on pooling AMSR-E soil moisture estimates during the calendar years 2003 and 2004. Over the TX/OK portion of the transect (boxes 1 to 4 in Fig. 1), all R_{value} coefficients are significantly greater than zero (at a 95% uncertainty threshold) for both products in every transect box. However, AMSR-E$_{LSMEM}$ retrievals demonstrate consistently larger R_{value} coefficients than comparable AMSR-E$_{NASA}$ retrievals. This difference implies that AMSR-E$_{LSMEM}$ retrievals correlate better with actual soil moisture conditions and are of relatively greater value for land surface modeling applications within
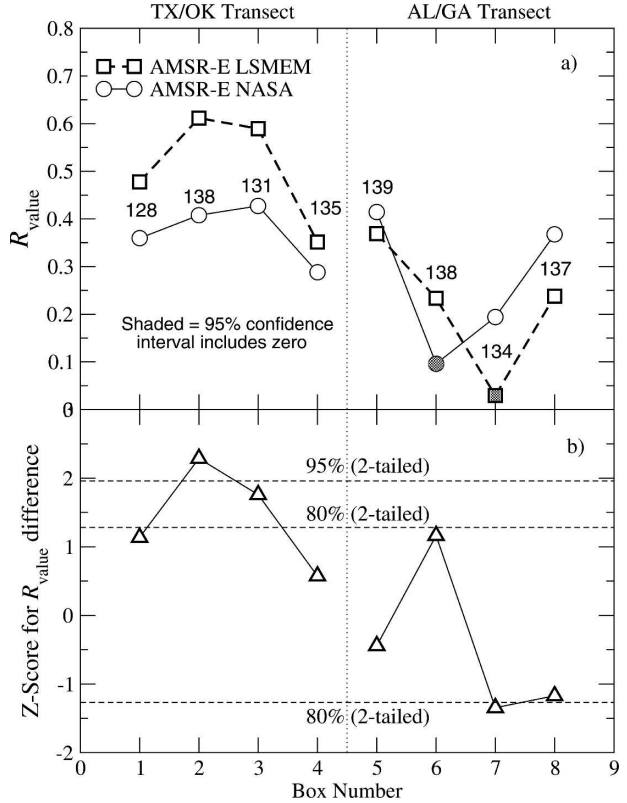

FIG. 7. (a) R_{value} coefficients and (b) the statistical significance of coefficient differences for both AMSR-E-based soil moisture products along the two transects defined in Fig. 1. The numbers in (a) represent the number of independent pentads used to calculate R_{value}.

these sites (Fig. 4). Because of the relatively short historical record of AMSR-E observations, R_{value} differences between AMSR-E products are statistically significant for only one of the four boxes (Fig. 7b). Better statistical power is obtained by assuming spatially independent errors and lumping correlation results from all four TX/OK transect boxes. After such spatial lumping, R_{value} differences between the two AMSR-E products are statistically significant at a 95% threshold level (Table 1).

Because of heavier vegetation amounts and more pronounced topography, spaceborne soil moisture retrieval is relatively more difficult for the AL/GA transect (boxes 5 to 8 in Fig. 1). This difficulty is reflected in smaller R_{value} coefficients for the AL/GA transect relative to the TX/OK transect (Fig. 7a). Nevertheless, R_{value} magnitudes (for both products) are significantly greater than zero for three of the four AL/GA transect boxes (Fig. 7a). In addition, the relative superiority of the products is reversed relative to the TX/OK transect. Along the AL/GA transect, the AMSR-E$_{NASA}$ product generally produces larger R_{value}

TABLE 1. Lumped R_{value} estimates, number of pentads used to calculate lumped R_{value} estimates (N), and the two-tailed statistical significance of R_{value} differences (i.e., LSMEM vs NASA or USDA vs NASA) for the case of pooling all four transect boxes.

Product	Transect	R_{value}	N	Significance
AMSR-E$_{NASA}$	TX/OK	0.37	532	95%
AMSR-E$_{LSMEM}$	TX/OK	0.51		
AMSR-E$_{NASA}$	AL/GA	0.27	548	<50%
AMSR-E$_{LSMEM}$	AL/GA	0.22		
TMI$_{USDA}$	TX/OK	0.30	1889	99.5%
TMI$_{LSMEM}$	TX/OK	0.42		
TMI$_{USDA}$	AL/GA	0.32	1922	93%
TMI$_{LSMEM}$	AL/GA	0.24		

FIG. 8. (a) R_{value} coefficients and (b) the statistical significance of coefficient differences for both TMI-based soil moisture products along the two transects defined in Fig. 1. The numbers in (a) represent the number of independent pentads used to calculate R_{value}.

coefficients than the AMSR-E$_{LSMEM}$ retrievals. However, the statistical significance of these differences is low (Fig. 7b)—even when AL/GA transect boxes are lumped (Table 1).

Figure 8 is identical to Fig. 7, except that it displays results for soil moisture products derived from the TMI sensor (rather than AMSR-E). These results have the benefit of a longer historical period (7 yr versus only 2 for AMSR-E) and slightly better temporal frequency. Over the TX/OK transect, assimilation of TMI$_{LSMEM}$ soil moisture retrievals results in a stronger correlation of filter increments with antecedent rainfall errors (i.e., higher R_{value} coefficients) than the assimilation of TMI$_{USDA}$ retrievals (Fig. 8a). The R_{value} coefficient differences are significant at a 95% threshold level for two boxes and an 80% threshold level for the other two (Fig. 8b). When transect boxes are spatially lumped, the significance of the pooled differences rises to the 99.5% confidence level (Table 1).

As with the AMSR-E soil moisture products, the relative ranking of the TMI soil moisture products reverses when moving from the TX/OK to the AL/GA transect. Larger R_{value} coefficients are associated with TMI$_{USDA}$ soil moisture retrievals than comparable TMI$_{LSMEM}$ retrievals over the length of the AL/GA transect. When transect boxes are spatially lumped, pooled differences are significant at a 93% confidence level (Table 1). In addition, the longer TMI heritage makes it possible to identify statistically significant value (i.e., R_{value} significantly larger than zero at the 95% confidence level) in both products for all four AL/GA transect boxes.

6. Discussion

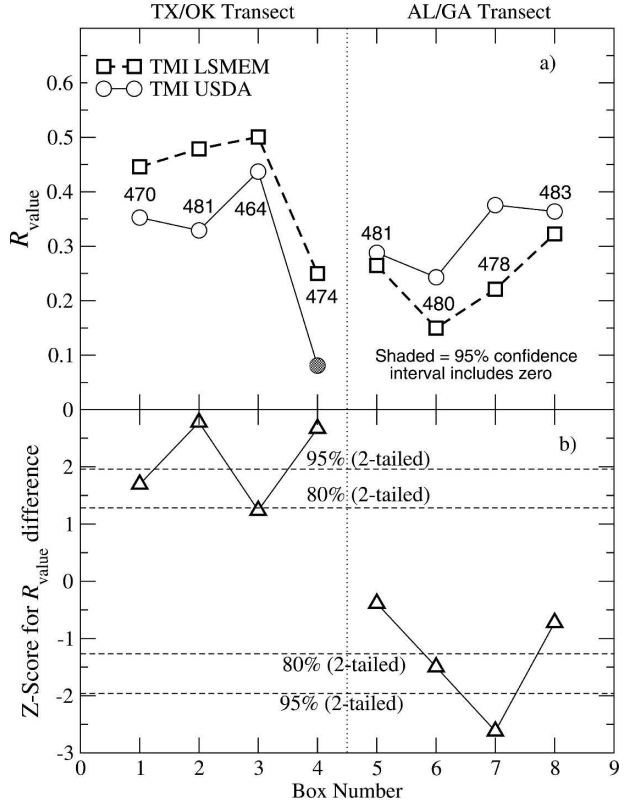Results in Figs. 7 and 8 can be partially explained by methodological differences among the various retrieval approaches. For instance, the largest difference between the AMSR-E$_{LSMEM}$ and AMSR-E$_{NASA}$ approaches examined in Fig. 7 is that the LSMEM approach utilizes only horizontally polarized brightness temperatures ($T_{B,H}$) while the Njoku/NASA algorithm is based on multipolarization $T_{B,H}$ and $T_{B,V}$ observations. The use of $T_{B,V}$ measurements allows the Njoku/NASA approach to simultaneously solve for both vegetation water content (W) and soil moisture. In contrast, the single-polarization LSMEM approach relies on ancillary visible remote sensing products to independently estimate W magnitudes required for soil moisture retrieval. Consequently, the ancillary data needs of the AMSR-E$_{NASA}$ product are less than those of the AMSR-E$_{LSMEM}$ product. Nevertheless, Fig. 7 demonstrates that, at least over the more lightly vegetated TX/OK transect, it is preferable to rely on these ancillary W estimates rather than incorporate $T_{B,V}$ observations and attempt to solve for W (and soil moisture) using a multipolarization approach. The relative advantage of the single-polarization approach, however, disappears over the more heavily vegetated AL/GA transect. One potential explanation for this reversal is

that the constitutive relationships used to estimate W from ancillary visible-based observations are more accurate for crop and grassland environments (e.g., the TX/OK transect) and tend to break down over areas with more complex canopy structures and/or dense woody vegetation.

The largest difference between the TMI_{LSMEM} and TMI_{USDA} approaches examined in Fig. 8 lies in the source of land surface temperature (T_S) fields used to retrieve surface soil moisture. The Gao/LSMEM approach is based on incorporating independent land surface T_S estimates from a land surface model running as part of the NLDAS project while the Bindlish/U.S. Department of Agriculture (USDA) approach attempts to retrieve T_S using $T_{B,V}$ observations. Both approaches estimate W using visible remote sensing products. Over the TX/OK transect, the use of the NLDAS T_S model product appears to provide the TMI_{LSMEM} product with a significant edge over the TMI_{USDA} product. However, this tendency reverses itself over the AL/GA transect. Particularly striking is the lack of a reduction in R_{value} between transects for the TMI_{USDA} approach (Table 1). Unlike the other three products, TMI_{USDA} R_{value} coefficients do not reflect relatively more difficult conditions for soil moisture remote sensing within the AL/GA transect.

Despite the general unsuitability of conditions along the AL/GA transect for soil moisture remote sensing, added value (i.e., statistically significant R_{value}) is found along its length for all four products. It should be noted that this added skill is calculated relative to the use of lower-quality GPCP-1DD rainfall data (higher-quality CPC rainfall data are intentionally withheld to serve as an independent source of evaluation data). The use of GPCP-1DD rainfall makes results indicative of added value obtainable in precipitation data–poor areas outside the United States. Consequently, absolute value results presented in Figs. 7 and 8 are best interpreted as test bed results that exploit the data-rich environment of the contiguous United States to reflect the added value of remote sensing observations for precipitation data–poor regions of the globe.

7. Summary and conclusions

Validation of global remote sensing products is typically based on the use of test bed sites in data-rich areas to characterize retrieval accuracy and value in higher-order application. Unfortunately, our ability to directly validate spaceborne soil moisture products against ground-based observations is currently limited by difficulties in maintaining soil moisture instrumentation networks and upscaling sparse point-scale observations

of highly variable soil moisture fields to spaceborne footprint scales (10–30 km). In this study we propose and apply a Kalman filter–based evaluation strategy that does not require the availability of ground-based soil moisture measurements and can be applied anywhere relatively high quality rain gauge observations are available (e.g., the contiguous United States). As a result, the approach greatly expands the geographic and temporal extent of potential ground test bed sites within which the value of remotely sensed soil moisture estimates can be assessed. In addition, the approach provides a quantitative measure of added value that is relative to the datum established by the accuracy of currently available global rainfall products and simple water balance modeling. This datum represents a critical benchmark that remotely sensed soil moisture products must improve upon in order to contribute value to global land surface modeling applications (Crow et al. 2005a).

A synthetic twin experiment establishes that the approach yields a metric (R_{value}), which is a well-defined function of both the underlying accuracy of the soil moisture retrievals, as well as the quality of rainfall observations used to calculate competing model-based soil moisture estimates (Fig. 4). This interpretation is not undermined by benchmark rainfall errors, temporal gaps in soil moisture retrievals, or the misspecification of model parameters (Fig. 5). Application to real datasets (Figs. 7 and 8) allows for hypothesis testing concerning the added value of various remote sensing soil moisture products for land surface modeling applications. Results indicate that even retrievals from non-optimal, X-band frequency sensors over heavily vegetated areas (i.e., the AL/GA transect) significantly enhance the quality of soil moisture predictions derived from a simple water balance model and the spaceborne GPCC-1DD precipitation dataset. Over a large fraction of the earth's surface, such satellite-based precipitation datasets provide the only available source of rainfall data. Consequently, this result offers strong support for the added utility of spaceborne soil moisture observations for soil moisture monitoring in precipitation data–poor regions of the world. In particular, the presence of detectable skill at X band along the AL/GA transect bodes well for future spaceborne missions based on lower-frequency L-band measurements [e.g., the European Space Agency Soil Moisture and Ocean Salinity (SMOS) mission (Kerr et al. 2001)]. Any skill present at X band within the AL/GA transect should be enhanced by longer-wavelength observations better suited for the penetration of dense vegetation canopies.

Results also provide valuable feedback for the design of spaceborne soil moisture retrieval strategies. Figures

7 and 8 suggest that single-polarization approaches that utilize ancillary W and T_S data from outside sources are superior over the lightly vegetated TX/OK transect. However, a multipolarization approach that incorporates both $T_{B,H}$ and $T_{B,V}$ measurements in an effort to reduce dependence on ancillary W or T_S observations is generally advantageous for the more heavily vegetated GA/AL transect. This lack of geographic consistency suggests that considerable merit exists in future satellite missions carrying multiple types of soil moisture retrieval algorithms forward in their data stream. More careful analysis will be required to confirm these results. Nevertheless, they provide an example of the type of retrieval algorithm design feedback afforded by the approach. For this preliminary analysis, our test bed is limited to two transects in the southern United States. However, no practical barriers exist for expanding the approach over broader precipitation data–rich areas of North America, Europe, and Asia.

In closing, two caveats are worth noting. First, R_{value} results presented here are based on a very simple API land surface model. The approach could potentially be modified such that (1) is replaced by a more physically realistic land surface model. Such a modification would allow for consideration of a wider range of land surface modeling error and not simply the impact of precipitation uncertainty. However, with increased modeling complexity also comes greater ambiguity concerning the interpretation of data assimilation results, a need for a more complex data assimilation approach, and, ultimately, more technical and practical barriers for the adoption of the methodology by remote sensing dataset developers and users. Future work will address the impact of more complex land surface modeling methodologies and potential trade-offs between model complexity and the tractability of the approach.

Finally, it is important to note that this approach is intended to complement, not replace, traditional validation techniques for remotely sensed soil moisture. The approach is somewhat application dependent in its emphasis on land surface modeling and, consequently, would not likely fully satisfy current NASA or European Space Agency programmatic requirements for remote sensing product validation. However, by using more easily acquired ground-based rainfall measurements as an effective proxy for less widely available soil moisture measurements, it expands our ability to objectively assess—and ultimately improve—the quality of spaceborne soil moisture products.

REFERENCES

Bindlish, R., T. J. Jackson, E. F. Wood, H. Gao, P. Starks, D. Bosch, and V. Lakshmi, 2003: Soil moisture estimates from TRMM Microwave Imager observations over the southern United States. *Remote Sens. Environ.,* **85,** 507–515.

Cosgrove, B. A., and Coauthors, 2003: Real-time and retrospective forcing in the North American Land Data Assimilation System (NLDAS) project. *J. Geophys. Res.,* **108,** 8842, doi:10.1029/2002JD003118.

Cosh, M. H., T. J. Jackson, R. Bindlish, and J. H. Prueger, 2004: Watershed scale temporal persistence of soil moisture and its role in validating satellite estimates. *Remote Sens. Environ.,* **92,** 427–435.

Crow, W. T., R. Bindlish, and T. J. Jackson, 2005a: The added value of spaceborne passive microwave soil moisture retrievals for forecasting rainfall-runoff partitioning. *Geophys. Res. Lett.,* **32,** L18401, doi:10.1029/2005GL023543.

——, R. D. Koster, R. H. Reichle, and H. O. Sharif, 2005b: Relevance of time-varying and time-invariant retrieval error sources on the utility of spaceborne soil moisture products. *Geophys. Res. Lett.,* **32,** L24405, doi:10.1029/2005GL024889.

Dee, D. P., 1995: On-line estimation of error covariance parameters for atmospheric data assimilation. *Mon. Wea. Rev.,* **123,** 1128–1145.

Drusch, M., E. F. Wood, and T. J. Jackson, 2001: Vegetation and atmospheric corrections for the soil moisture retrieval from passive microwave remote sensing data: Results from the 1997 Southern Great Plains Hydrology Experiment. *J. Hydrometeor.,* **2,** 181–192.

Famiglietti, J. S., and Coauthors, 1999: Ground-based investigation of soil moisture variability within remote sensing footprints during the Southern Great Plains (SGP97) Hydrology Experiment. *Water Resour. Res.,* **35,** 1839–1851.

Gao, H., E. F. Wood, M. Drusch, W. T. Crow, and T. J. Jackson, 2004: Using a microwave emission model to estimate soil moisture from ESTAR observations during SGP99. *J. Hydrometeor.,* **5,** 49–63.

——, ——, ——, T. Jackson, and R. Bindlish, 2006: Using TRMM/TMI to retrieve soil moisture over the southern United States from 1998 to 2002. *J. Hydrometeor.,* **7,** 23–38.

Groisman, P. Y., and D. R. Legates, 1994: The accuracy of United States precipitation data. *Bull. Amer. Meteor. Soc.,* **75,** 215–227.

Huffman, G. J., R. F. Adler, M. M. Morrissey, D. T. Bolvin, S. Curtis, R. Joyce, B. McGavock, and J. Susskind, 2001: Global precipitation at one-degree daily resolution from mulitisatellite observations. *J. Hydrometeor.,* **2,** 36–50.

Jackson, T. J., D. M. Le Vine, A. Y. Hsu, A. Oldak, P. J. Starks, C. T. Swift, J. Isham, and M. Haken, 1999: Soil moisture mapping at regional scales using microwave radiometry: The

Southern Great Plains Hydrology Experiment. *IEEE Trans. Geosci. Remote Sens.,* **37,** 2136–2151.

Jacobs, J. M., B. P. Mohanty, E. C. Hsu, and D. Miller, 2004: Field scale variability and similarity of soil moisture. *Remote Sens. Environ.,* **92,** 436–446.

Kerr, Y. H., P. Waldteufel, J.-P. Wigneron, J.-M. Martinuzzi, J. Font, and M. Berger, 2001: Soil moisture retrieval from space: The soil moisture and ocean salinity mission (SMOS). *IEEE Trans. Geosci. Remote Sens.,* **39,** 1729–1735.

Leese, J., T. J. Jackson, A. Pitman, and P. Dirmeyer, 2001: GEWEX/BAHC international workshop on soil moisture monitoring, analysis and prediction for hydrometeorological and hydroclimatological applications. *Bull. Amer. Meteor. Soc.,* **82,** 1423–1430.

McPhee, J., and S. Margulis, 2005: Validation and error characterization of GPCP-1DD precipitation product over the contiguous United States. *J. Hydrometeor.,* **6,** 441–459.

Njoku, E. G., T. J. Jackson, V. Lakshmi, T. Chan, and S. V. Nghiem, 2003: Soil moisture retrieval from AMSR-E. *IEEE Trans. Geosci. Remote Sens.,* **41,** 215–229.

Reichle, R. H., and R. D. Koster, 2005: Global assimilation of satellite surface soil moisture retrievals into the NASA Catchment land surface model. *Geophys. Res. Lett.,* **32,** L02404, doi:10.1029/2004GL021700.

——, D. B. McLaughlin, and D. Entekhabi, 2002: Hydrologic data assimilation with the ensemble Kalman filter. *Mon. Wea. Rev.,* **130,** 103–114.